ACS APPLIED MATERIALS & INTERFACES

Research Article

www.acsami.org

# Polybenzimidazole Block Copolymers for Fuel Cell: Synthesis and Studies of Block Length Effects on Nanophase Separation, Mechanical Properties, and Proton Conductivity of PEM

Sudhangshu Maity and Tushar Jana*

School of Chemistry University of Hyderabad Hyderabad 500046, India

Supporting Information

**ABSTRACT:** A series of *meta*-polybenzimidazole-*block*-*para*-polybenzimidazole (*m*-PBI-*b*-*p*-PBI), segmented block copolymers of PBI, were synthesized with various structural motifs and block lengths by condensing the diamine terminated *meta*-PBI (*m*-PBI-Am) and acid terminated *para*-PBI (*p*-PBI-Ac) oligomers. NMR studies and existence of two distinct glass transition temperatures ($T_g$), obtained from dynamical mechanical analysis (DMA) results, unequivocally confirmed the formation of block copolymer structure through the current polymerization methodology. Appropriate and careful selection of oligomers chain length enabled us to tailor the block length of block copolymers and also to make varieties of structural motifs. Increasingly distinct $T_g$ peaks with higher block length of segmented block structure attributed the decrease in phase mixing between the *meta*-PBI and *para*-PBI blocks, which in turn resulted into nanophase segregated domains. The proton conductivities of proton exchange membrane (PEM) developed from phosphoric acid (PA) doped block copolymer membranes were found to be increasing substantially with increasing block length of copolymers even though PA loading of these membranes did not alter appreciably with varying block length. For example when molecular weight ($M_n$) of blocks were increased from 1000 to 5500 then the proton conductivities at 160 °C of resulting copolymers increased from 0.05 to 0.11 S/cm. Higher block length induced nanophase separation between the blocks by creating less morphological barrier within the block which facilitated the movement of the proton in the block and hence resulting higher proton conductivity of the PEM. The structural varieties also influenced the phase separation and proton conductivity. In comparison to meta−para random copolymers reported earlier, the current meta−para segmented block copolymers were found to be more suitable for PBI-based PEM.

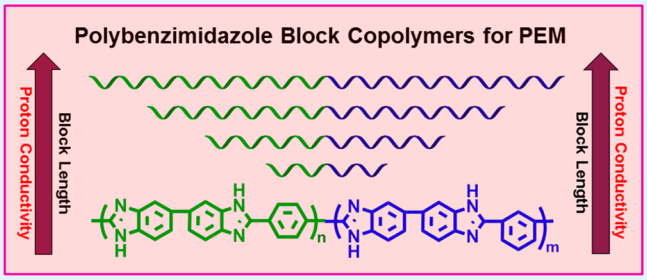


**KEYWORDS:** *polybenzimidazole, block copolymer, proton exchange membrane, proton conductivity, fuel cell*

## INTRODUCTION

Recently, research toward the development of polymeric membrane, which can be used as high temperature polymer electrolyte membrane (PEM) in fuel cell has gained considerable interests in the scientific community because of its several advantages compared to traditional PEMs which are only suitable for low operating temperature (<100 °C).[1−7] Among large number of polymeric systems which have been developed for this purpose, phosphoric acid (PA)-doped polybenzimidazole (PBI) has been found to be the most attractive because of their very high thermo-mechanical stability, resistance to chemical and long-term durability.[1−4,8−12]

With regard to the use of PA loaded PBI as PEM, several aspects of PBI chemistry have been studied thoroughly in last ten years. Few aspects among these which are often highlighted in the literature are solubility and hence processability issues of PBI, thermal and mechanical stability of PBI, acid loading capability, proton conductivity and especially the thermo-mechanical stability of PA doped PBI membrane in particular when PA loading is high.[13−17] Another important drawback which is also pointed out to be as one of the bottlenecks for the use in PEM is the durability of PA doped membrane since PA can readily leach out from the membrane and thereby reducing the membrane proton conducting character.[18−20]

To address the solubility problem, several varieties of PBI structures have been suggested.[21−25] However, many of them failed to enhance the solubility or even it improves, resulting membranes obtained from these new structures display inferior properties compared to traditional PBI as PEM. Recently, we have reported a new type of PBI called pyridine based PBI (Py-PBI),[26] which was synthesized from an alternative, inexpensive tetraamine monomer called 2,6-bis(3′,4′-diaminophenyl)-4-phenylpyridine (Py-TAB), which has very high solubility and as well as enhanced proton conducting character compared to traditional PBI. Other synthetic methods, which have been adapted very often to increase the processability, are grafting the alkyl or functionalized alkyl

Received: January 30, 2014
Accepted: April 8, 2014
Published: April 8, 2014

   dx.doi.org/10.1021/am500668c | ACS Appl. Mater. Interfaces 2014, 6, 6851−6864

chain in the PBI backbone[14,21,22,24] by substituting in the imidazole ring. However, these approaches also have many disadvantages.

In regard to the development and fabrication of PA-doped PBI membrane with workable thermomechanical stability, high PA loading and high proton conductivity several approaches have been explored in literature, recently several reviews have summarized all these methods.[1−4] Very often following four methods have been adapted and these are (1) synthesis of new PBI structures which include structural varieties in homopolymers and copolymers,[9−11,22,24,26−32] (2) development of novel fabrication method,[10,12,33−37] (3) preparation of nanocomposites of PBI with inorganic fillers such as clay, silica particles, nanotubes, graphene, etc.,[38−41] and (4) making blend with another polymer,[42−45] which helps to obtain the desired property as mentioned above. All these approaches of making PA-doped PBI membrane with high PA loading and conductivity without comprising thermo mechanical properties are extensively studied by us and many other groups.

Recently, synthesis of PBI copolymers increasingly becoming important since copolymer structure offers opportunities to improve the properties and especially the PA doped PBI membrane properties.[27−32,46−52] Majority of the literature reports are on the random copolymer of two or three different types of PBI. Among these random copolymers of meta-connected PBI and para-connected PBI are very significant since chemical structure-wise they are same, however their linkage with imidazole are different which makes them isomeric structure.[31] It has been pointed out that PA doped *para*-PBI shows higher conductivity than *meta*-PBI.[3,12,26] However, *para*-PBI has very low solubility and hence processability. Therefore, a combination of *meta*- and *para*-PBI can result into processable material and as well as good proton conducting PEM can be fabricated. With this background, earlier we had synthesized meta/para random copolymers.[31] However, we found that the conductivity did not improve as per our expectations. Hence, it became necessary for us to come up with new structural strategies.

It has been reported that the blocks of multiblock structure can easily phase separate into two domains which enhances the internal connectivity within the block and hence resulting in higher conductivity.[53−56] In literature only few reports are available on multiblock copolymers of PBI with poly(arylene ether sulfone)[38] and Benicewicz et al.[59] reported segmented block copolymer of sulfonated PBI with *para*-PBI. All of these reports highlighted increase in proton conductivity and argued that the nanophase segregation of blocks as the cause for higher conductivity. Keeping this background of nanophase separation of block structure and absence of meta/para block copolymer in the literature, we planned to synthesize *meta*-PBI-*block*-*para*-PBI (*m*-PBI-*b*-*p*-PBI) segmented block copolymers and study the effect of each block length on the phase separation and hence on the proton conductivities. We also attempted to build several structural varieties (motifs) of segmented block copolymers and study their influences on the properties of PEM obtained from these segmented block copolymers.

## EXPERIMENTAL SECTION

All the information about the materials used in this study, membrane fabrication method from the synthesized *m*-PBI-*b*-*p*-PBIs and the experimental methods of all the characterization techniques which include molecular weight measurements by viscosity and proton NMR analysis, thermogravimetric analysis (TGA) and dynamic mechanical analysis (DMA) for all the *m*-PBI-*b*-*p*-PBIs polymers are described in the Supporting Information. The $H_3PO_4$ doping level and the proton conductivity measurements of *m*-PBI-*b*-*p*-PBIs membranes are also discussed in the Supporting Information.

**Table 1. Monomer Mole Ratios and Molecular Weights of Synthesized Diamine- (Meta) and Acid-Terminated (Para) PBI Oligomers**

| diamine-terminated oligomer (*m*-PBI-Am) | | | acid-terminated oligomer (*p*-PBI-Ac) | | |
|---|---|---|---|---|---|
| TAB/IPA (mole ratio) | IV (dL/g)[a] | $M_n$ (g/mol)[b] | TAB/TPA (mole ratio) | IV (dL/g)[a] | $M_n$ (g/mol)[b] |
| 1.06:1 | 0.59 | 5500 | 1:1.06 | 0.54 | 5200 |
| 1.09:1 | 0.47 | 4300 | 1:1.09 | 0.43 | 4100 |
| 1.14:1 | 0.32 | 3100 | 1:1.14 | 0.35 | 3300 |
| 1.20:1 | 0.22 | 2100 | 1:1.20 | 0.23 | 2200 |
| 1.25:1 | 0.12 | 1000 | 1:1.25 | 0.11 | 1100 |

[a]Inherent viscosity (IV) determined from 0.2 g/dL oligomers solution in conc. $H_2SO_4$ (98%) at 30 °C. [b]Determined by $^1$H NMR end group analysis.

**Synthesis of Oligomers and Segmented Block Copolymers.** *Synthesis of Meta-Connected Diamine-Terminated Polybenzimidazole Oligomers.* Polycondensation of 3,3′4,4′-tetraaminobiphenyl (TAB) and isophthalic acid (IPA) monomers in polyphosphoric acid (PPA, 115%) medium was carried out to synthesize meta-connected diamine-terminated poly[2,2′-(*m*-phenylene)-5,5′-benzimidazole] oligomers (abbreviated as *m*-PBI-Am). We have conducted five sets of reactions by varying the relative mols ratios of TAB and IPA, and all the reactions were in 100 g scale. In all the cases total monomer concentration (TMC) at the beginning of the reaction was kept constant at 5 wt %. The mole ratio of TAB and IPA were altered to get the variable molecular weight of the resulting oligomers. We kept the fixed IPA mole ratio at 1.00 and systematically varied the TAB mole ratios from 1.06 to 1.25 as seen in Table 1. The reactions were carried out as follows: all reactions of different mols of TAB and IPA were taken into a three neck flask with 100 g PPA for diamine terminated oligomers synthesis and the reactions were carried out for 12 h at 190 °C. After the polymerization, the viscous oligomer solutions were slowly poured into the deionized water and washed with deionized water several times. Then dilute solution of ammonium hydroxide solution was added to neutralize the excess phosphoric acid. The oligomers were filtered and washed with ethanol several times and dried in vacuum oven for 3 days at 60 °C to remove the solvents completely. This reaction scheme is shown in Scheme 1.

*Synthesis of Para-Connected Acid-Terminated Polybenzimidazole Oligomers.* Para-connected acid-terminated poly[2,2′-(*p*-phenylene)-5,5′-benzimidazole] oligomers (abbreviated as *p*-PBI-Ac) were synthesized by condensing TAB and terephthalic acid (TPA) monomers in PPA medium. Here also we have carried out five sets of reactions by varying TAB and TPA mole ratio, and all are in 100 g scale and the total monomer concentrations (TMC) were kept constant at 3.5 wt %. We have varied the mole ratio of TAB and TPA to alter the molecular weight of oligomers. We have kept the fixed TAB mole ratio at 1.00 and varied the TPA mole ratio from 1.06 to 1.25 as seen in Table 1. All reactions of different mols of TAB and TPA were taken into a three neck flask with 100 g PPA for acid terminated oligomers synthesis and the reaction were carried out for 6−8 h at 190 °C. After the polymerization, the viscous oligomer solutions were slowly poured in to the deionized water and washed with deionized water several times. Then dilute solution of ammonium hydroxide was added to neutralize the excess phosphoric acid. The oligomers were filtered and washed with ethanol several times and dried in vacuum oven for 3 days at 60 °C to remove the solvents completely. Scheme 2 shows the reaction scheme.

*Synthesis of Segmented Block Copolymers of Polybenzimidazole.* Segmented block copolymers of PBI were synthesized by polycondensation (coupling) reactions of diamine (*m*-PBI-Am) and acid (*p*-PBI-Ac) terminated oligomers in PPA medium which resulted into *meta*-polybenzimidazole-*block*-*para*-polybenzimidazole (abbreviated as *m*-PBI-*b*-*p*-PBI). Three different types of segmented block copolymers

Scheme 1. Synthesis of Meta-Connected Diamine-Terminated Polybenzimidazole (*m*-PBI-Am) Oligomer

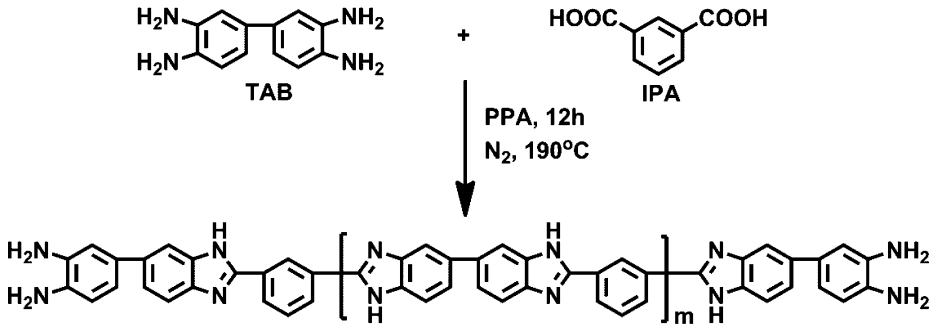


Diamine terminated *meta*-polybenzimidazole oligomer (*m*-PBI-Am)

Scheme 2. Synthesis of Para-Connected Acid-Terminated Polybenzimidazole (*p*-PBI-Ac) Oligomer

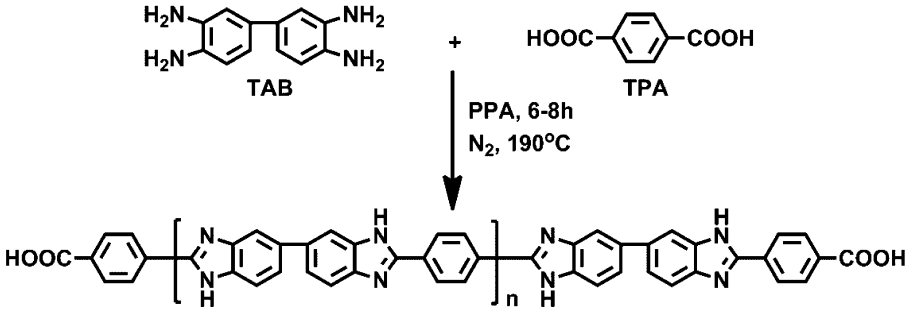


Acid terminated *para*-polybenzimidazole oligomer (*p*-PBI-Ac)

Scheme 3. Synthesis of Segmented Block Copolymers of Polybenzimidazole (*m*-PBI-*b*-*p*-PBI)

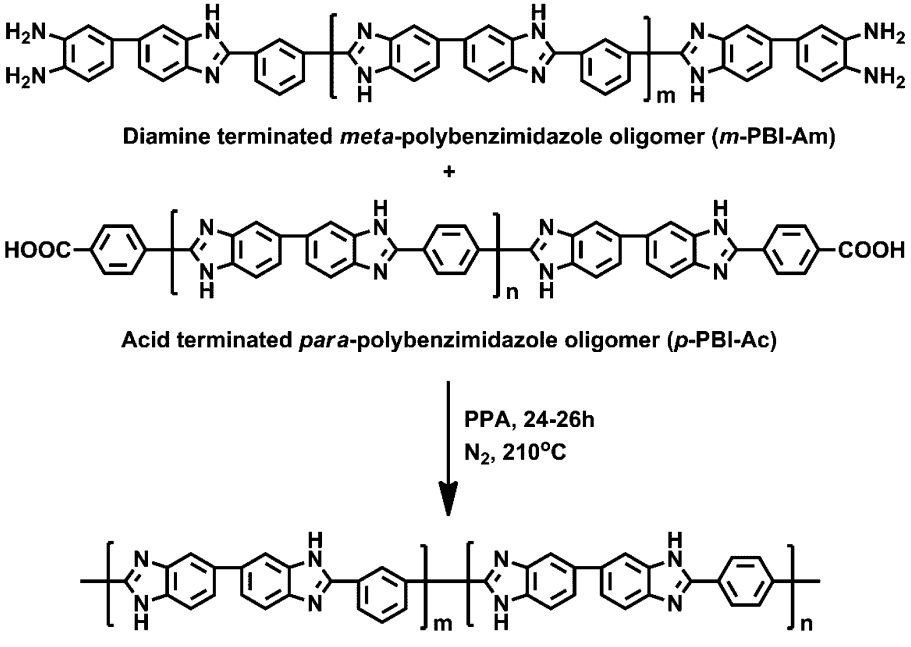


*meta*-polybenzimidazole-*block*-*para*-polybenzimidazole (*m*-PBI-*b*-*p*-PBI)

were synthesized and these are (I) ($Am_{fix}$-*b*-$Ac_{vary}$), in this we varied the block length of acid terminated oligomer with the fixed diamine terminated oligomer, (II) ($Am_{vary}$-*b*-$Ac_{fix}$), in this case we varied the diamine terminated oligomer with the fixed acid terminated oligomer and (III) ($Am_{equal}$-*b*-$Ac_{equal}$) where we took equal block length of diamine terminated and acid terminate oligomers. In case of block copolymer of $Am_{fix}$-*b*-$Ac_{vary}$ (case I), we have taken the highest molecular weight of diamine terminated oligomer ($M_n$ = 5500, Table 1), and in case of $Am_{vary}$-*b*-$Ac_{fix}$, the highest molecular weight of acid terminated oligomer ($M_n$ = 5200, Table 1) was chosen. The detail reactions recipes are summarized in Results and Discussion section (Table 3). We have taken the diamine and acid terminated PBI oligomers weight according to their end group analysis to maintain their stoichiometric balance. End group analysis technique by $^1$H NMR was


dx.doi.org/10.1021/am500668c | ACS Appl. Mater. Interfaces 2014, 6, 6851−6864

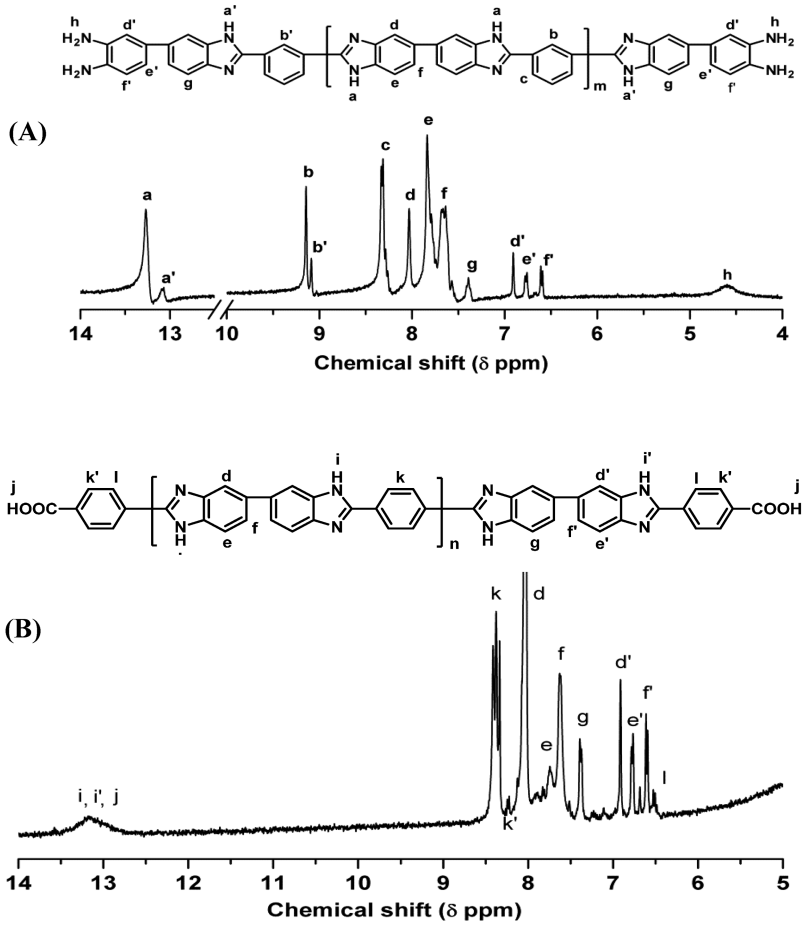


**Figure 1.** [1]H NMR spectra of (A) diamine terminated *meta*-polybenzimidazole oligomer (*m*-PBI-Am) (B) acid terminated *para*-polybenzimidazole oligomer (*p*-PBI-Ac). Peaks assignments and chemical structures of oligomers are also shown in the figure. All spectra were recorded using DMSO-$d_6$ as NMR solvent.

used to calculate the molecular weight of the oligomers.[57,58] All segmented block copolymers syntheses were carried in 100 g scale and total monomer concentrations were kept at 4 wt %. Polymerizations were carried out as follows: the synthesized oligomers with appropriate stoichiometry were taken in a three neck flask and connect with sealed over headed mechanical stirrer and the reaction was kept at 210 °C for 24−26 h with continuous nitrogen purging. After the complete polymerization, the viscous polymer solutions were slowly poured into the deionized water and washed several times. Then ammonium hydroxide solution was added to neutralize the excess phosphoric acid. The polymers were filtered and washed with deionized water several times and dried in vacuum oven for 3 days at 100 °C to remove the solvents completely. The synthesis of segmented block copolymers of PBI is represented in Scheme 3.

## RESULTS AND DISCUSSION

**Synthesis of Polybenzimidazole Oligomers.** Since in this work, we wish to prepare PBI block copolymers hence first we need to synthesize oligomeric blocks, which further can be connected by condensation (coupling) to build the block copolymer structure. To get the block copolymer structure of PBI, we need to have diamine terminated PBI oligomeric structure and acid terminated PBI oligomeric structure which upon condensing can produce block PBI structure. As shown in Schemes 1 and 2, we have prepared diamine terminated *meta*-polybenzimidazole (*m*-PBI-Am) oligomer and acid terminated *para*-polybenzimidazole (*p*-PBI-Ac) oligomer by the condensation reaction TAB with IPA and TPA, respectively in PPA. It is expected that further condensation of these two oligomers structure will produce block PBI structure in which one block would be meta-connected structure and other would be para-connected structure. To get the terminal functionalities in oligomers we have used stoichiometric imbalance method in the reaction mixture as shown in Table 1. For diamine termination higher amount TAB was taken and similarly for acid termination higher amount of acid was taken. Since we also would like to see the effect of block lengths in the final properties of PBI block copolymers, therefore it is necessary to build different chain length oligomeric structures. To do so, we have varied the mole ratios of IPA and TPA with the TAB. For meta-connected diamine-terminated PBI oligomers, we have varied the mole ratio of TAB 1 to 1.25 with a fixed 1 mol ratio of IPA and for *p*-PBI-Ac oligomer TPA mole ratio 1 to 1.25 with a fixed 1 mol ratio of TAB were altered. From Table 1 it is clear that with increasing the stoichiometric imbalances; the molecular weight (inherent viscosity, IV and $M_n$) of both the diamine and acid terminated oligomers gradually decrease.

The proton NMR spectra of both *m*-PBI-Am and *p*-PBI-Ac oligomers are shown in Figure 1 with their peak assignments. The structures match very well with the spectral data. In both the oligomers, the terminal peaks are assigned as shown in Figure 1. In case of *m*-PBI-Am (Figure 1A), the terminal peaks of oligomers are assigned by a′, b′, d′, e′, f′, g and h. The other peaks are assigned as nonterminal peaks. The terminal imidazole proton peaks are appeared at 13.08 ppm designated

as a′, terminal aromatic proton appears in between 6.56 and 7.46 ppm assigned as d′, e′, f′, g, and terminal amine peak appear at 4.61 ppm numbered as h. Similarly in case of *p*-PBI-Ac (Figure 1B), in addition to nonterminal peaks, all terminal peaks are assigned as d′, e′, f′, g, i′, j, k′, and l. In which d′, e′, f′, and g represent the terminal aromatic protons as shown in Figure 1A. The i′ peak at ∼13.12 ppm represents the imidazole proton and j at ∼13.12 ppm is assigned as terminal carboxylic proton. It must be noted that the peaks at ∼13.12 ppm (denoted as i, i′, j) are broad in nature and this is due to overlap of carboxylic and imidazole proton peaks.

The number-average molecular weight ($M_n$) of diamine and acid terminated oligomers are calculated from the end group analysis by peak integration of $^1$H NMR spectra using methods as described in the Supporting Information, which is similar to method reported earlier.[57,58] The molecular weights ($M_n$) of diamine terminated oligomers are varied from 1000 to 5500 and for acid-terminated oligomers 1100 to 5200 (Table 1). $M_n$ values also follow the similar trend as inherent viscosity (IV) values in both the cases; with increasing stoichiometric imbalance $M_n$ decreases. The $M_n$ increases with increasing IV values as per the expectation in both the cases. Linear relationships between IV and $M_n$ are observed for both the cases (*m*-PBI-Am and *p*-PBI-Ac) when a log−log plots are drawn between IV and $M_n$ (Supporting Information Figure 1) which confirmed the successful control of molecular weights for both the blocks.[55−58]

It is important to note that, we have prepared diamine-terminated oligomer using IPA with TAB and acid-terminated oligomer using TPA with TAB (Schemes 1 and 2 and Table 1). The question can be asked why not vice versa i.e. TPA for diamine termination and IPA for acid termination and why we are so particular about it? In fact, this should have been a natural choice since our earlier studies indicated formation of diamine terminated oligomeric species as a major intermediate when TPA and TAB condensation takes place owing to the low solubility of TPA in PPA. We also attributed this as a cause for formation of high molecular weight (MW) PBI whenever a para-connected diacid (such as TPA) is used.[26,30,31] In this study, initially, we indeed attempted to make diamine oligomer using TPA and acid oligomer using IPA and the results are shown in Table 2. However, we observe that MW (IV values)

**Table 2. Monomer Mole Ratios and Inherent Viscosity of Synthesized Diamine- (Para) and Acid (Meta)-Terminated PBI Oligomers**

| acid-terminated oligomer (Am) | | diamine-terminated oligomer (Ac) | |
|---|---|---|---|
| TAB/IPA (mole ratio) | IV (dL/g)[a] | TAB/TPA (mole ratio) | IV (dL/g)[a] |
| 1:1.014 | 0.71 | 1.014:1 | 3.01 |
| 1:1.065 | 0.21 | 1.065:1 | 0.81 |
| 1:1.114 | 0.03 | 1.114:1 | 0.61 |

[a]Determined from 0.2 g/dL oligomers solution in conc. $H_2SO_4$ (98%) at 30 °C.

of diamine-terminated oligomers are always higher than the acid-terminated oligomer (Table 2) even though stoichiometric imbalance are quite similar. This is quite obvious as the reason stated above and as per our earlier observation.[26,30,31] Therefore, we do not have good control over the MW (chain size) of both the oligomers, which will not allow us to build the final block structure with several varieties. Hence, we opted the reverse, that is, IPA for diamine-terminated and TPA for acid-terminated as discussed and shown in Schemes 1 and 2 and Table 1, where we have very good control over both oligomers' MW, and hence, we can build blocky PBI structure of several varieties which will be discussed in next section. The reason why TPA produced lower MW acid-terminated oligomer compared to that of the diamine-terminated (Table 1) is that acid termination is preferred instead of diamine termination because of high acid stoichiometry.

**Synthesis of Segmented Block Copolymer of Polybenzimidazoles.** *meta*-Polybenzimidazole-*block*-*para*-polybenzimidazole (*m*-PBI-*block*-*p*-PBI) is synthesized by condensing equal moles of diamine-terminated *meta*-PBI and acid-terminated *para*-PBI oligomers in PPA medium for 24 h as shown in Scheme 3. The stoichiometric balance (1:1 mol) of *p*-PBI-Ac and *m*-PBI-Am oligomers in the polymerization feed are maintained in all the block copolymer synthesis based on the calculated stoichiometry of oligomers obtained from end group analysis using $^1$H NMR spectra. It is expected that this condensation of oligomers will yield blocky structure of PBI. A careful analysis of $^1$H NMR spectra further clarified the formation of segmented block PBI. $^1$H NMR spectra of representative segmented block PBI is shown in Figure 2 along

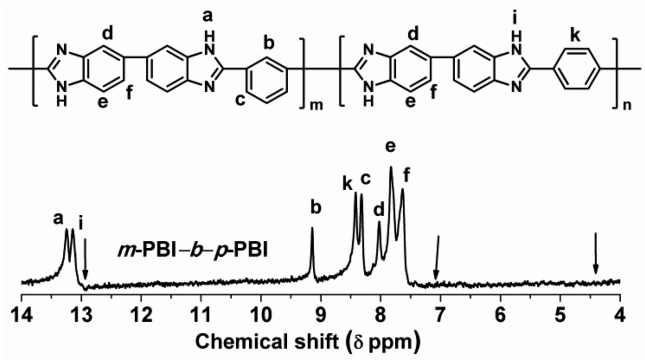


**Figure 2.** $^1$H NMR spectra of *meta*-PBI-*block*-*para*-PBI block copolymer. Peaks assignments and chemical structure of block copolymer is shown in the figure. Spectrum was recorded using DMSO-$d_6$ as NMR solvent. Arrow indicating the disappearance of terminal peaks of oligomer because of formation of block PBI copolymer.

with block structure. The peak assignments of the segmented block structures are also represented in the figure. A comparison of Figure 2 spectra with oligomeric spectra shown in Figure 1 clearly proves the formation of block structure. In case of *m*-PBI-Am oligomer (Figure 1A), the peaks of terminal diamine protons (h) appear at 4.61 ppm and terminal imidazole peak is seen at 13.08 ppm (a′). Similarly all the terminal aromatic peaks (b′, d′, e′, f′, g) are also clearly distinguishable (Figure 1A). Similarly in case of *p*-PBI-Ac oligomer (Figure 1B) the terminal acid (j), and imidazole peaks (i′) are identified as broad peaks along with regular peak. The remaining terminal aromatic (d′, e′, f′, g, k′, l) peaks are seen as in case of *m*-PBI-Am. The block copolymer *m*-PBI-*block*-*p*-PBI, $^1$H NMR spectra matches well with the expected structure as shown in Figure 2. The complete disappearance of terminal protons signals of both oligomers [imidazole (a′, i′), amine (h), acid (j), and aromatic (b′, d′, e′, f′, g, k′, l)] as shown by the arrow in Figure 2 clearly indicates the ring closer of the condensation polymerization and hence the formation of block copolymer of PBI. The all other peaks are indicated in the figure clearly

**Table 3. Oligomer Combinations and Molecular Weights of Synthesized Segmented Block Copolymer of Polybenzimidazoles and the Schematic Structures of Block Copolymers**

| Oligomers I.V. (dL/g) *m*-PBI-Am : *p*-PBI-Ac | Block copolymer I.V. (dL/g)[a] | Copolymer composition[b] (*meta*/*para*) | Schematic structure[c] |
|---|---|---|---|
| Fixed diamine-*block*-variable acids copolymer ($Am_{fix}$-*b*-$Ac_{vary}$) | | | |
| 0.59 : 0.11 | 2.01 | - | |
| 0.59 : 0.23 | 1.42 | 63.60/36.40 | |
| 0.59 : 0.35 | 0.87 | 60.44/39.56 | |
| 0.59 : 0.43 | 0.87 | 52.75/47.25 | |
| Variable diamine-*block*-fixed acid copolymer ($Am_{vary}$-*b*-$Ac_{fix}$) | | | |
| 0.12 : 0.54 | 1.62 | - | |
| 0.22 : 0.54 | 1.08 | 37.18/62.82 | |
| 0.32 : 0.54 | 1.06 | - | |
| 0.47 : 0.54 | 0.97 | 43.75/56.25 | |
| Equal diamine-*block*-equal acid copolymer ($Am_{equal}$-*b*-$Ac_{equal}$) | | | |
| 0.12 : 0.11 | 0.47 | - | |
| 0.22 : 0.23 | 1.28 | 49.95/50.05 | |
| 0.32 : 0.35 | 0.75 | - | |
| 0.47 : 0.43 | 1.33 | 51.79/48.21 | |
| 0.59 : 0.54 | 1.37 | 52.90/47.10 | |

[a] Determined from 0.2 g/dL polymers solution in conc. $H_2SO_4$ (98%) at 30 °C.
[b] Determined by $^1$H NMR peak integration using equation 1.
[c] ∿∿ = *m*-PBI-Am and ∿∿ = *p*-PBI-Ac

attributes and agrees with block PBI structure as shown in Scheme 3.

The above discussion and Figure 2 clearly prove the formation of segmented block PBI copolymer structure upon condensation of diamine and acid terminated PBI oligomers. It is to be noted from Table 1 that we have synthesized both types of PBI oligomers with variable chain length (molecular weight). Therefore, we can utilized the various combination of these variable chain length oligomers to build the different types of segmented block PBI structures as shown in Table 3. The schematic structures of blocks are shown in last column of Table 3. There varieties of block PBI structures are prepared and these are (I) fixed diamine-*block*-variable acids ($Am_{fix}$-*b*-$Ac_{vary}$), (II) variable diamine-*block*-fixed acid ($Am_{vary}$-*b*-$Ac_{fix}$) and (III) equal diamine-*block*-equal acid ($Am_{equal}$-*b*-$Ac_{equal}$). In case of (I) ($Am_{fix}$-*b*-$Ac_{vary}$); we have chosen the highest molecular weight of diamine terminated *m*-PBI oligomer and varied the acid terminated *p*-PBI oligomers molecular weight. Similarly, in case of (II) ($Am_{vary}$-*b*-$Ac_{fix}$); we have chosen the highest molecular weight of acid terminated *p*-PBI oligomer and varied the molecular weight of diamine terminated *m*-PBI oligomers. But in case of (III) ($Am_{equal}$-*b*-$Ac_{equal}$); similar molecular weight of both oligomer are chosen, however, their size are vary equally from one polymer to another.

In both the cases of fixed amine- and acid-terminated block copolymer of PBI; the molecular weight gradually decreases with the increasing of counter oligomers molecular weight (Table 3). This could be due to the reactivity of counter oligomers which gradually decreases with the increasing the molecular weight of the oligomers due the different chain length of oligomers which do not allow the longer chain length to react readily. But in case of the equal ammine and acid terminate block (case III) copolymer, because of the equal length of molecular weight; they have the same reactivity and the condensation reaction takes place readily.

The proton NMR spectra of all the three types of segmented block PBI structures with variable chain length of meta and para blocks are shown in Figure 3. The peaks assignments are also shown in the figure with the segmented block structure and schematic color coding. It must be carefully noted that the peaks, which are designated by a, b, c, are for the meta structure and similarly the peaks, which are assigned as i, k, are for the para structure of PBI.[27] As it can be seen that, in case of $Am_{fix}$-*b*-$Ac_{vary}$ (Figure 3B), the peaks (i, k) because of the para structure becomes stronger with increasing IV (molecular weight and chain length) of para block in the segmented block structure. Similarly, meta structure peaks (a, b, c) becomes more and more prominent in case of $Am_{vary}$-*b*-$Ac_{fix}$ (Figure 3C) with increasing IV of meta PBI oligomer. However, in case of $Am_{equal}$-*b*-$Ac_{equal}$ (Figure 3C), relative intensity of both meta and para peaks remain same, but peaks become more intense as we increase the chain length.

The para copolymer compositions (meta/para) in the segmented block structure are calculated from the integral ratio of proton peaks (a, b, c, i, k) intensities with help of following eq 1 and listed in Table 3. In case of $Am_{equal}$-*b*-$Ac_{equal}$ (Case III) samples the meta/*para* compositions are always approximately 50/50 irrespective of block length, which is in agreement with the feed meta/para composition (50/50). On the other hand, meta/para composition alters in other two types of block; the % of para increases with increasing block length (MW) of para connected acid terminated oligomer in case of $Am_{fix}$-*b*-$Ac_{vary}$ (case I); where as % of para decreases with increasing block length of amine terminated oligomer in case of $Am_{vary}$-*b*-$Ac_{fixed}$ (case II). These are simply due to the effect of corresponding block length which changes as we alter the molecular weight of oligomers.

$$\%\ \text{of para mole fraction in the copolymer} = \frac{I_i + I_k}{I_a + I_b + I_c + I_i + I_k} \quad (1)$$

**Thermal Stability.** We have carried out TGA analysis for all diamine- and acid-terminated oligomers, and the three sets of segmented block copolymers of PBI under continuous nitrogen flow from room temperature to 800 °C. Supporting Information Figure 2 and Figure 4 show the thermal degradation of the oligomers and block copolymers, respectively. It is clearly visible that all synthesized oligomers and block copolymers are highly thermally stable as per the expectation for PBI type polymers. The weight loss at the initial stage near 150 °C is occurring because of the loss of loosely hydrogen bonded water molecules, which are associated with the polymer backbone. The weight loss after 600 °C is due to the degradation of the benzimidazole group of the polymer backbone. Both in case of diamine and acid terminated oligomers; the thermal stability gradually increases

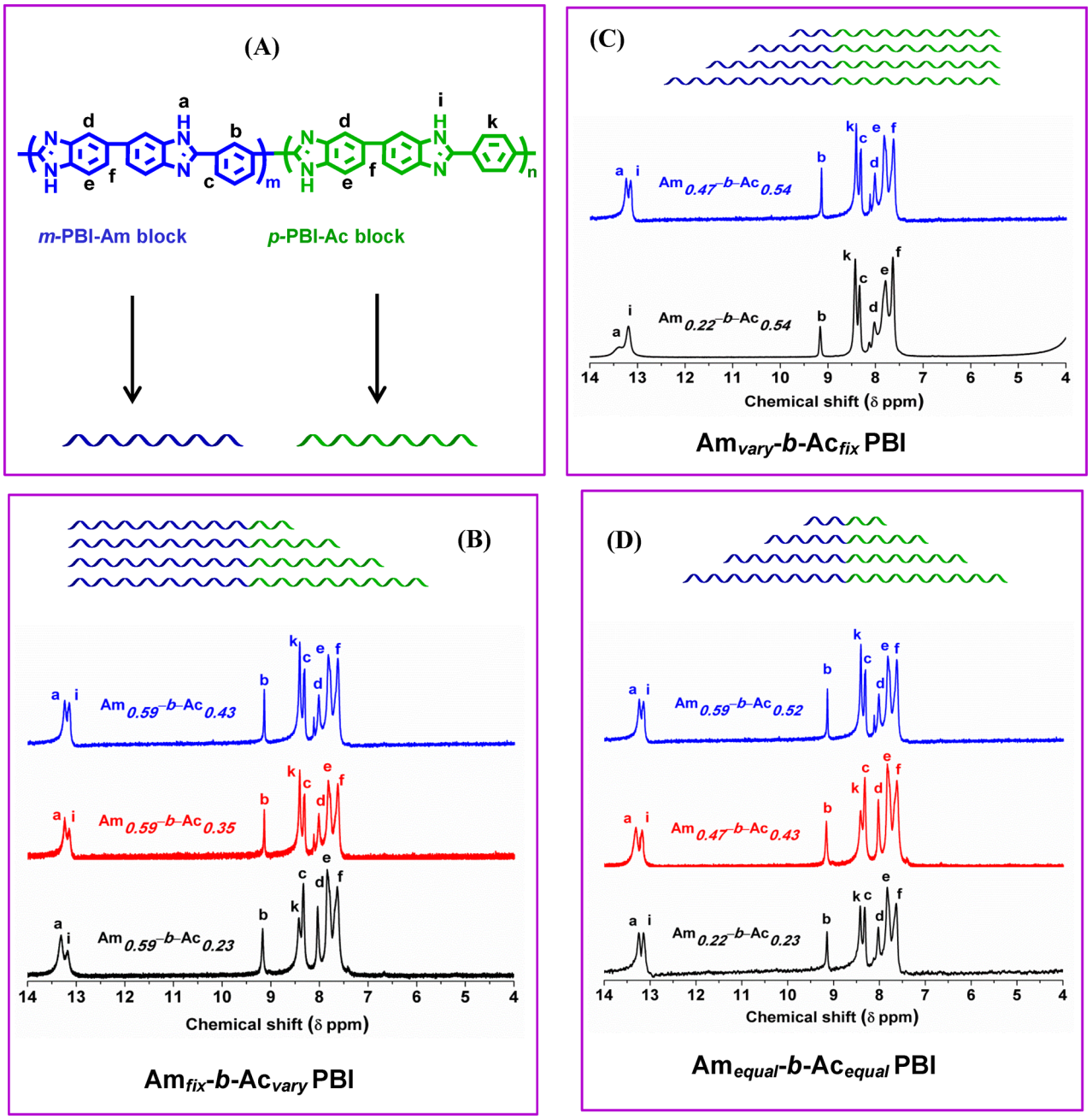


**Figure 3.** $^1$H NMR spectra of PBI segmented block copolymer of varieties of structures (as shown in Table 3): (A) a general block structure with peak assignments and schematic color coding for each block, (B) $Am_{fix}$-*b*-$Ac_{vary}$, (C) $Am_{vary}$-*b*-$Ac_{fix}$, and (D) $Am_{equal}$-*b*-$Ac_{equal}$. The data are recorded from DMSO-$d_6$. Schematic segmented block structures along with color coding are shown in each case with their spectra.

with increasing the molecular weight of oligomers (Supporting Information Figure 2).

The thermal stability of block copolymers are shown in Figure 4 display the dependence on the copolymer structure; for example in case of $Am_{fix}$-*b*-$Ac_{vary}$, the thermal stability decreases with increasing MW (chain length) of para-connected acid-terminated block (Figure 4A). We have found similar trend in case of $Am_{vary}$-*b*-$Ac_{fix}$, where thermal stability decreases with increasing MW of meta-connected block (Figure 4B). Therefore, it can be said that although block lengths are increasing in these two cases, however their thermal stability decrease and this is probably due to the decrease of the molecular weight (as seen from inherent viscosity values) of segmented block copolymer with increasing block length as showed in Table 3. But in case of the equal amine and acid terminated block copolymer (case III) we got the reverse results; thermal stability increases with increasing block length (Figure 4C). The molecular weight of the resulting block copolymer gradually increases with increasing both molecular weight of acid and amine terminated oligomers. This is because the molecular wight of the block copolymers increases with increasing the block length of both oligomers.

**Dynamic Mechanical Properties.** The temperature dependent various thermo-mechanical properties such as storage modulus ($E'$), loss modulus ($E''$) and tan $\delta$ of PBI segmented block copolymers are studied using DMA. The glass transition temperature ($T_g$) of all types of segmented block PBIs are obtained from temperature dependent plots of both $E''$ and tan $\delta$ as shown in Figure 5 and Supporting Information


dx.doi.org/10.1021/am500668c | ACS Appl. Mater. Interfaces 2014, 6, 6851−6864

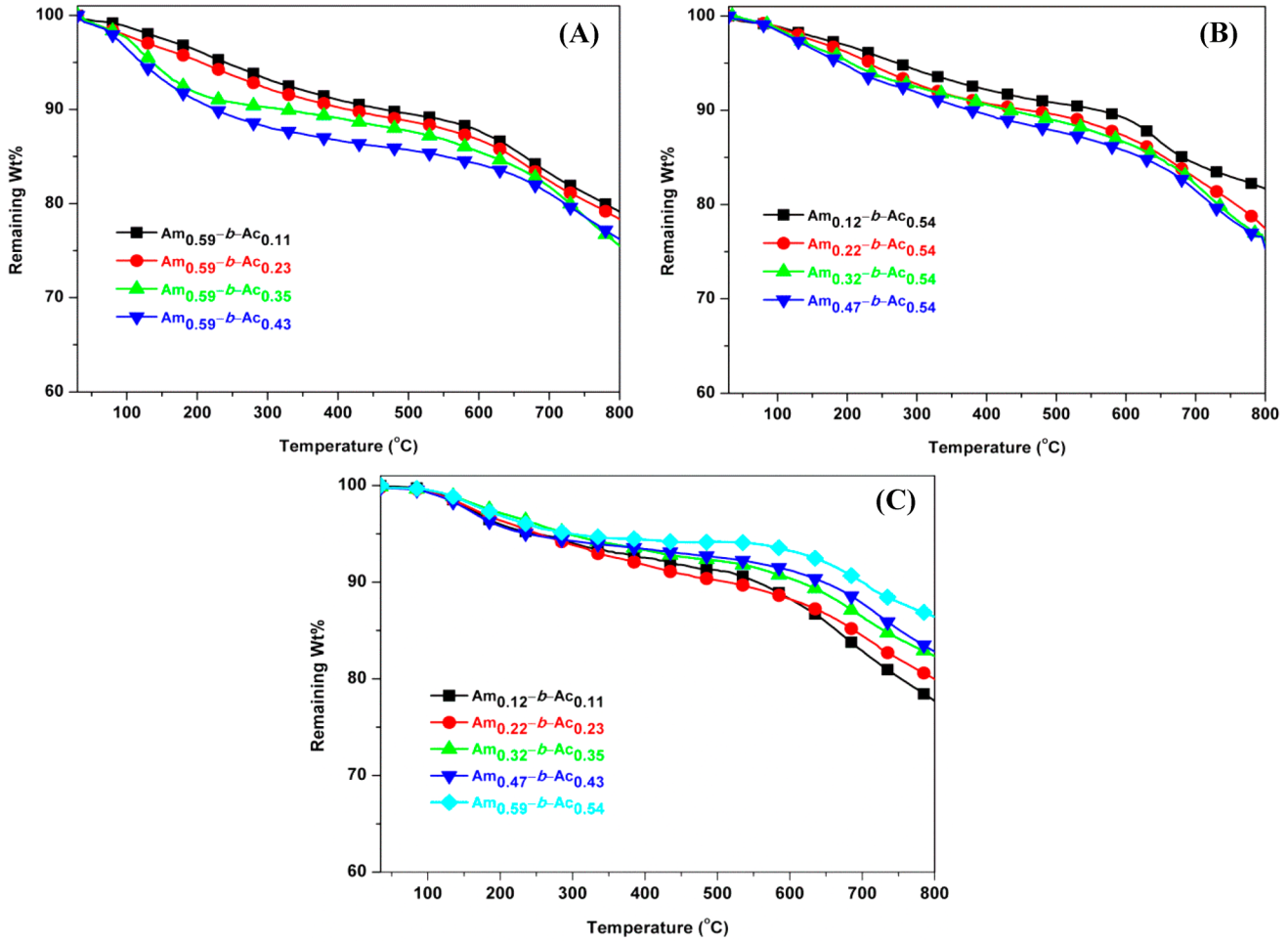


**Figure 4.** Thermogravimetric plots of (A) $Am_{fix}$-*b*-$Ac_{vary}$, (B) $Am_{vary}$-*b*-$Ac_{fix}$, and (C) $Am_{equal}$-*b*-$Ac_{equal}$ block copolymer of PBI in $N_2$ atmosphere at the heating rate of 10 °C/min.

Figure 3, respectively. All the samples display two distinct glass transition temperatures, attributing the formation of segmented block copolymer structures.[57,58] All the $T_g$ values for all samples are tabulated in Table 4. It has been reported by us and several other authors earlier that *para*-PBI $T_g$ is lower than *meta*-PBI $T_g$ owing to the symmetrical structure of *para*-PBI.[1−3,27−32] Based on this experience, we have identified the lower temperature transitions as $T_g$ for para block (acid terminated) and higher temperature transition as $T_g$ of meta block (diamine terminated).

In case of fixed diamine terminated segmented block copolymer ($Am_{fix}$-*b*-$Ac_{vary}$, case I); the $T_g$ of fixed meta block length does not change much, it is only 5−7 °C [395−402 °C (tan $\delta$ plot) and 380−385 °C ($E''$ plot)], however with increasing the chain length of para acid block part $T_g$ increases significantly (20−30 °C) from 329 to 349 °C (tan $\delta$ plot) and from 298 to 317 °C ($E''$ plot) as shown in Supporting Information Figure 3A, Figure 5A, and Table 4. Similarly, in case of fixed acid terminated block copolymer ($Am_{vary}$-*b*-$Ac_{fix}$, case II); the $T_g$ of fixed para block length does not change that much, but with increasing the chain length of meta diamine block part $T_g$ increases significantly as shown in Supporting Information Figure 3B, Figure 5B, and Table 4. But in case of equal acid and equal diamine terminated block copolymers ($Am_{equal}$-*b*-$Ac_{equal}$, Case III), we have got two $T_g$ and both are increasing with increasing meta and para block length (Supporting Information Figure 3C, Figure 5C, and Table 4). This is due to both meta and para having similar size block chain length and hence with increasing size (chain length) their $T_g$ increases in a similar manner. It is reported in the literature that with increasing the block lengths the glass transition temperature gradually increases.[57,58] Here we also found the same trend. From the above discussion of DMA study, it is clear that the $T_g$ variations depend on the block length and the type of the block structure. Since the molecular weight (MW) of block copolymer varies depending on the block length and the structure; hence, there could be some effect of MW on $T_g$ as well. However, the trend of $T_g$ variations as shown in Table 4 does not seem to reflect the MW dependence on $T_g$. Therefore, in summary, it is confirmed that the synthesized copolymer structure is segmented block structure and the $T_g$ values varies with nature of block and especially with the block length.

It must be noted that with increasing block length, the two $T_g$ peaks which are assigned to two separate blocks (meta and para) become increasingly distinct and prominent in all the three sets of samples in both $E'$ and tan $\delta$ plots as shown in Figure 5 and Supporting Information Figure 3, respectively. This attributes that with increasing block length the degree of mixing between the two blocks decreases and hence resulted into higher degree of phase separation. Hence, at higher block length nanophase segregation of two blocks are more prominent. This nanophase separation is most distinct in case

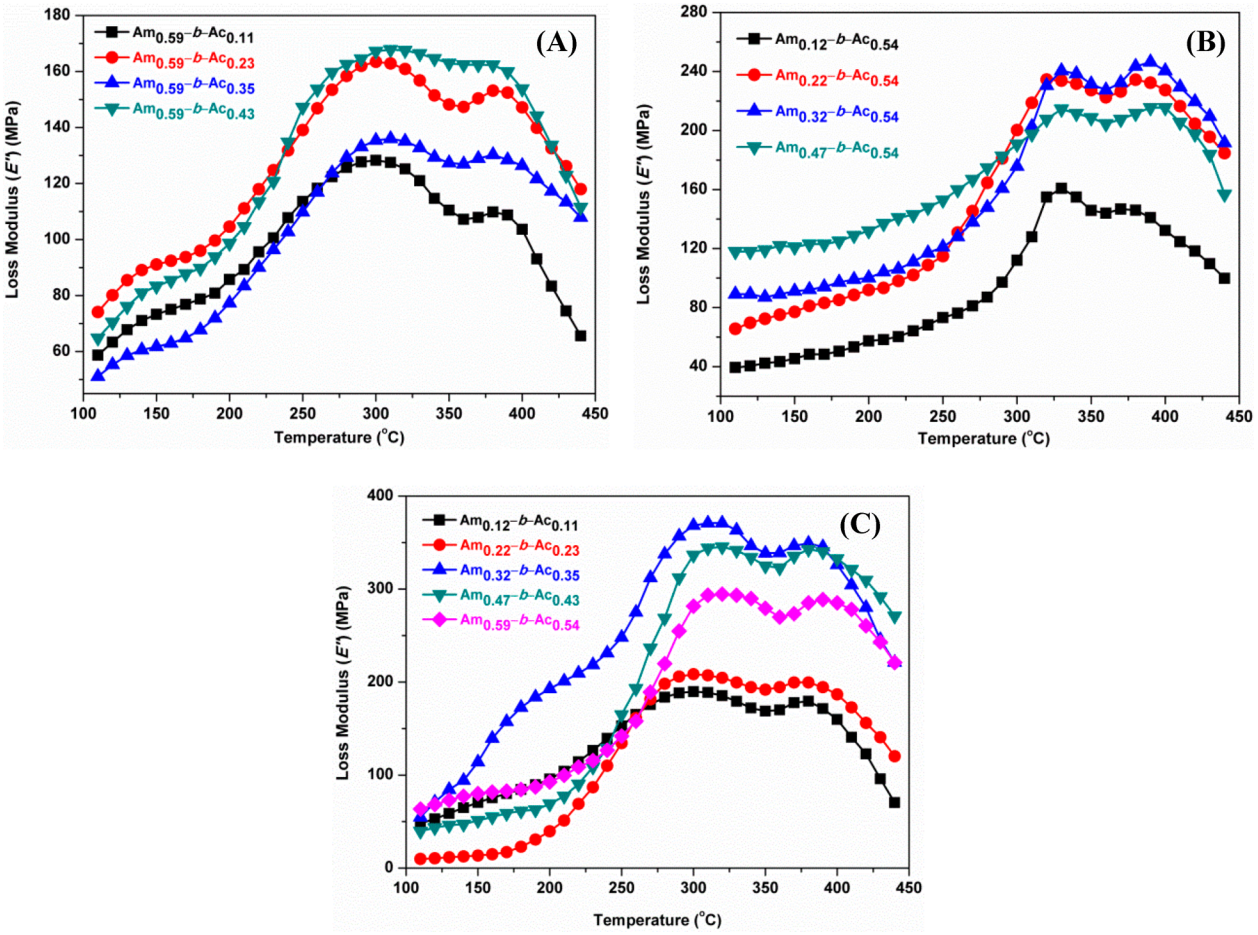


**Figure 5.** Loss modulus ($E''$) against temperature plots of PBI block copolymers: (A) fixed diamine terminated with varied acid terminated ($Am_{fix}$-*b*-$Ac_{vary}$), (B) fixed acid terminated with varied diamine terminated ($Am_{vary}$-*b*-$Ac_{fix}$), and (C) equal diamine and acid terminated ($Am_{equal}$-*b*-$Ac_{equal}$). These results are obtained from DMA study at the heating rate of 4 °C/min.

of $Am_{equal}$-*b*-$Ac_{equal}$ block and they are different in nature for other two blocks as well.[55−58]

Figure 6 displays the storage modulus ($E'$) variation as a function of temperature for all types of samples. In all the cases with increasing block length $E'$ values are increasing in the entire temperature range even though in case of $Am_{fix}$-*b*-$Ac_{vary}$ and $Am_{vary}$-*b*-$Ac_{fix}$ MW decreases with increasing block length as shown in Table 3 in earlier section. It also interesting to note that, the percent of increase in $E'$ values is not only depends on the block length but also significantly relies on the block structure as seen from Figure 6 plots.

**Phosphoric Acid Loading.** Table 5 tabulated the phosphoric acid (PA) doping level for all three types of segmented block copolymers when the membranes are doped by dipping into 85% (14.6 M) $H_3PO_4$ for 7 days. The PA doping level for all the samples varies between 8 and 11 mol per PBI repeat unit. We do not observe any definite conclusive trend with increasing block length, molecular weight of the polymer and the type of segmented block structures. The little variations are may be due to the meta/para composition variation from one copolymer to another. These measured doping levels of segmented block copolymer are comparable with the literature reported doping level of *meta*- and *para*-PBI polymers when doped using similar condition (85% PA for 7 days).[1−3,27−32,60] It has been reported earlier also that membranes of *meta*- and *para*-PBI obtained from solvent casting method do not display much difference in acid loading. However, the *meta*- and *para*-PBI membranes obtained from direct casting method by sol−gel process (known as PPA process), developed by Benicewicz et al., exhibit significant difference in PA loading.[3,12] We also made meta−para random PBI copolymer in which meta/para composition is 50/50 and measured PA loading of this sample is ∼10 mol/PBI repeat unit. Hence, it is clear that block structure of PBI not influence the PA loading character of the membrane which is justifiable since PA molecules interact with all the imidazole groups in a same manner irrespective of their nanophase separation or segregation.

Although it might be argued that with increasing block length more PA loading should have taken place which indeed true to some extent in all the cases. However, it must be noted that especially in case of $Am_{fix}$-*b*-$Ac_{vary}$ and $Am_{vary}$-*b*-$Ac_{fix}$, the MW (IV values) of copolymers decrease with increasing block length (Table 3), which in turn can decrease the PA loading, but observed PA loading for these two copolymers do not decrease indicating that blocks structure might have facilitated the absorption of PA owing to their phase separated morphology. However, in case of $Am_{equal}$-*b*-$Ac_{equal}$ the increase in PA loading is more prominent than other two block structure since MW in this case does not decrease with increasing block length unlike other two cases.

**Table 4. Glass Transition Temperatures ($T_g$) of *m*-PBI-*b*-*p*-PBI Copolymers Obtained from DMA Study**

| block polymer | $T_g$ from $E''$ (°C) | | $T_g$ from tan $\delta$ (°C) | |
|---|---|---|---|---|
| | amine block (meta) | acid block (para) | amine block (meta) | acid block (para) |
| fixed diamine-*block*-variable acid block copolymer ($Am_{fix}$-*b*-$Ac_{vary}$) | | | | |
| $Am_{0.59}$–*b*–$Ac_{0.11}$ | 383 | 298 | 395 | 329 |
| $Am_{0.59}$–*b*–$Ac_{0.23}$ | 385 | 306 | 398 | 338 |
| $Am_{0.59}$–*b*–$Ac_{0.35}$ | 380 | 311 | 397 | 342 |
| $Am_{0.59}$–*b*–$Ac_{0.43}$ | 382 | 317 | 402 | 349 |
| variable diamine-*block*-fixed acid block copolymer ($Am_{vary}$-*b*-$Ac_{fix}$) | | | | |
| $Am_{0.12}$–*b*–$Ac_{0.54}$ | 375 | 330 | 393 | 359 |
| $Am_{0.22}$–*b*–$Ac_{0.54}$ | 381 | 326 | 397 | 360 |
| $Am_{0.32}$–*b*–$Ac_{0.54}$ | 390 | 334 | 405 | 365 |
| $Am_{0.47}$–*b*–$Ac_{0.54}$ | 399 | 331 | 417 | 364 |
| equal diamine-*block*-equal acid block copolymer ($Am_{equal}$-*b*-$Ac_{equal}$) | | | | |
| $Am_{0.12}$–*b*–$Ac_{0.11}$ | 377 | 300 | 400 | 326 |
| $Am_{0.22}$–*b*–$Ac_{0.23}$ | 381 | 306 | 408 | 336 |
| $Am_{0.32}$–*b*–$Ac_{0.35}$ | 385 | 314 | 403 | 344 |
| $Am_{0.47}$–*b*–$Ac_{0.43}$ | 391 | 319 | 417 | 351 |
| $Am_{0.59}$–*b*–$Ac_{0.54}$ | 399 | 327 | 420 | 354 |

Also, we have measured the dimensional changes (swelling ratio and increase in thickness) of the block copolymer membranes upon PA loading for 7 days and the data are included in Table 5. The results obtained are in good agreement with the earlier observation reported in the literature. Both the swelling ratio and thickness increase do not display any dependence on block length, molecular weight of the polymer and the type of segmented block structures (Table 5).

**Proton Conductivity.** The proton conductivity of acid doped membranes is the key property of high temperature polymer electrolyte membrane (PEM) since fuel cell efficiency directly related to the proton conductivity. The proton conductivity measurements were carried out from room temperature to 160 °C. The proton conductivity as a function of temperature of all the segmented block copolymer membranes are obtained from the Nyquist plots from the second heating measurement as discussed in the Experimental Section. All experiments have been carried out without any external humidification supply. The representative Nyquist plots obtained from the impedance measurements are shown in Supporting Information Figure 4. Figure 7 represents, the proton conductivity versus temperature plots for all three types of block copolymers. As mentioned in the previous section, all these membranes were doped by dipping into 85% PA ($H_3PO_4$) for 7 days and their PA loading are not considerably different as seen from Table 5.

In all three cases of block copolymers proton conductivities increases with increasing temperature which are in good agreement with the behavior of PA doped PBI membrane as reported in the literature. From Figure 7, it is clearly evident

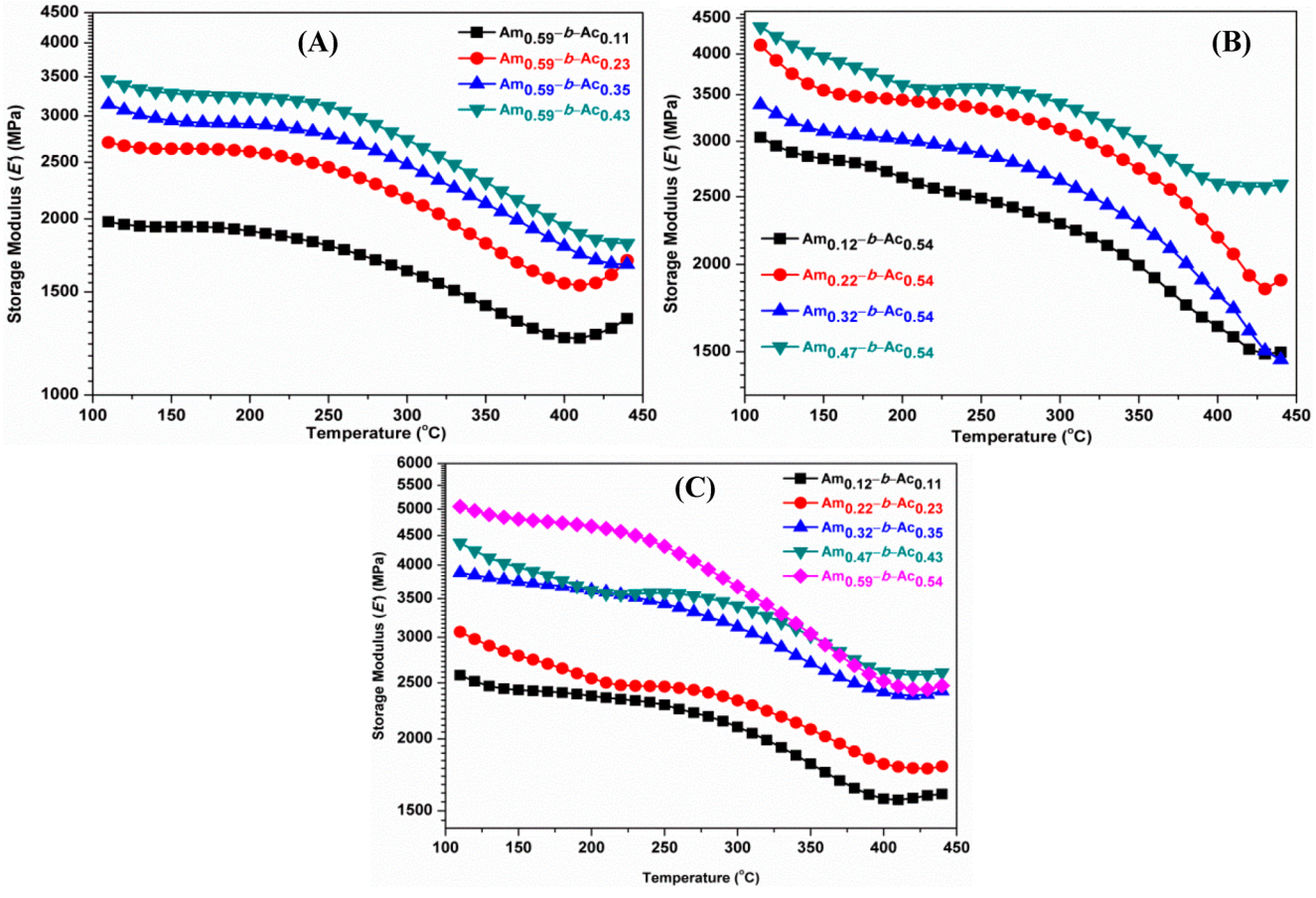


**Figure 6.** Storage modulus ($E'$) against temperature plots of PBI block copolymers: (A) fixed diamine terminated with varied acid terminated ($Am_{fix}$-*b*-$Ac_{vary}$), (B) fixed acid terminated with varied diamine terminated ($Am_{vary}$-*b*-$Ac_{fix}$), and (C) equal diamine and acid terminated ($Am_{equal}$-*b*-$Ac_{equal}$). These results are obtained from DMA study at the heating rate of 4 °C/min.

**Table 5. Swelling and Phosphoric Acid (PA) Loading Data of All Three Types of Segmented Block PBI Copolymers after Dipping in PA for 7 Days**[a]

| block polymer | swelling ratio (%) | thickness increase (%) | PA (mols/PBI repeat unit) |
|---|---|---|---|
| fixed diamine-*block*-variable acid block copolymer ($Am_{fix}$-*b*-$Ac_{vary}$) | | | |
| $Am_{0.59}$–*b*–$Ac_{0.11}$ | 6.50 (0.26) | 34.81 (2.19) | 7.77 (1.59) |
| $Am_{0.59}$–*b*–$Ac_{0.23}$ | 6.60 (0.02) | 35.67 (0.97) | 8.66 (0.16) |
| $Am_{0.59}$–*b*–$Ac_{0.35}$ | 6.66 (0.39) | 35.79 (0.80) | 8.97 (0.10) |
| $Am_{0.59}$–*b*–$Ac_{0.43}$ | 7.02 (0.44) | 34.64 (5.44) | 9.88 (0.62) |
| variable diamine-*block*-fixed acid block copolymer ($Am_{vary}$-*b*-$Ac_{fix}$) | | | |
| $Am_{0.12}$–*b*–$Ac_{0.54}$ | 6.25 (0.19) | 35.41 (2.95) | 8.19 (0.46) |
| $Am_{0.22}$–*b*–$Ac_{0.54}$ | 6.37 (0.08) | 36.66 (4.71) | 9.05 (0.65) |
| $Am_{0.32}$–*b*–$Ac_{0.54}$ | | | 10.43 (0.36) |
| $Am_{0.47}$–*b*–$Ac_{0.54}$ | 6.55 (0.22) | 37.5 (0.03) | 9.55 (0.04) |
| equal diamine-*block*-equal acid block copolymer ($Am_{equal}$-*b*-$Ac_{equal}$) | | | |
| $Am_{0.12}$–*b*–$Ac_{0.11}$ | 6.17 (0.08) | 29.16 (5.89) | 8.42 (0.30) |
| $Am_{0.22}$–*b*–$Ac_{0.23}$ | 6.25 (0.07) | 35.00 (8.08) | 8.81 (0.25) |
| $Am_{0.32}$–*b*–$Ac_{0.35}$ | 6.28 (0.03) | 33.93 (12.62) | 10.81 (0.68) |
| $Am_{0.47}$–*b*–$Ac_{0.43}$ | 6.34 (0.04) | 38.88 (7.85) | 10.72 (0.01) |
| $Am_{0.59}$–*b*–$Ac_{0.54}$ | 6.34 (0.06) | 30.95 (3.65) | 11.64 (0.14) |

[a]The standard deviations are shown in the parentheses.

that in all the three cases proton conductivities in the entire temperature range increase with increasing block length. Also, it must be noted that the increase in conductivity with block length is most prominent in case of $Am_{equal}$-*b*-$Ac_{equal}$ copolymers (Figure 7C). In this case at 160 °C, the conductivity of smallest block length copolymer ($Am_{0.12}$-*b*-$Ac_{0.11}$) is 0.05 S/cm whereas largest block length copolymer ($Am_{0.59}$-*b*-$Ac_{0.54}$) display 0.11 S/cm (Figure 7C). Generally, proton conductivity of PBI based membrane increases with increasing PA loadings. In the current segmented block copolymers, PA loadings are almost similar, then question can be asked why proton conductivity varying with chain length and structural motif of copolymers. The other interesting observation that in case of random meta/para copolymer where meta/para composition is 50/50 and also the acid loading is ~10 mol/PBI repeat unit, the conductivity is much lower than the other 50/50 block copolymer as shown in Figure 7D. At 160 °C random meta/para copolymer coductivity is 0.04 S/cm whereas segmented block meta/para coplymer conductivity is much higher. Even the smallest block length sample conductivity is 0.05 S/cm which is higher than the random copolymer.

The higher proton conductivity of segmented block copolymer than random copolymer despite the similar PA loading, increase of proton conductivity with increasing block length although PA loading are same can be attributed to the formation of phase separated morphology with increasing block length[55,58] as observed from the DMA study (earlier section). It is known that para-structured PBI display higher proton conductivity than meta-structured PBI owing to its symmetrical nature.[1−3,26−32] In case of random meta/para (50/50) copolymer,

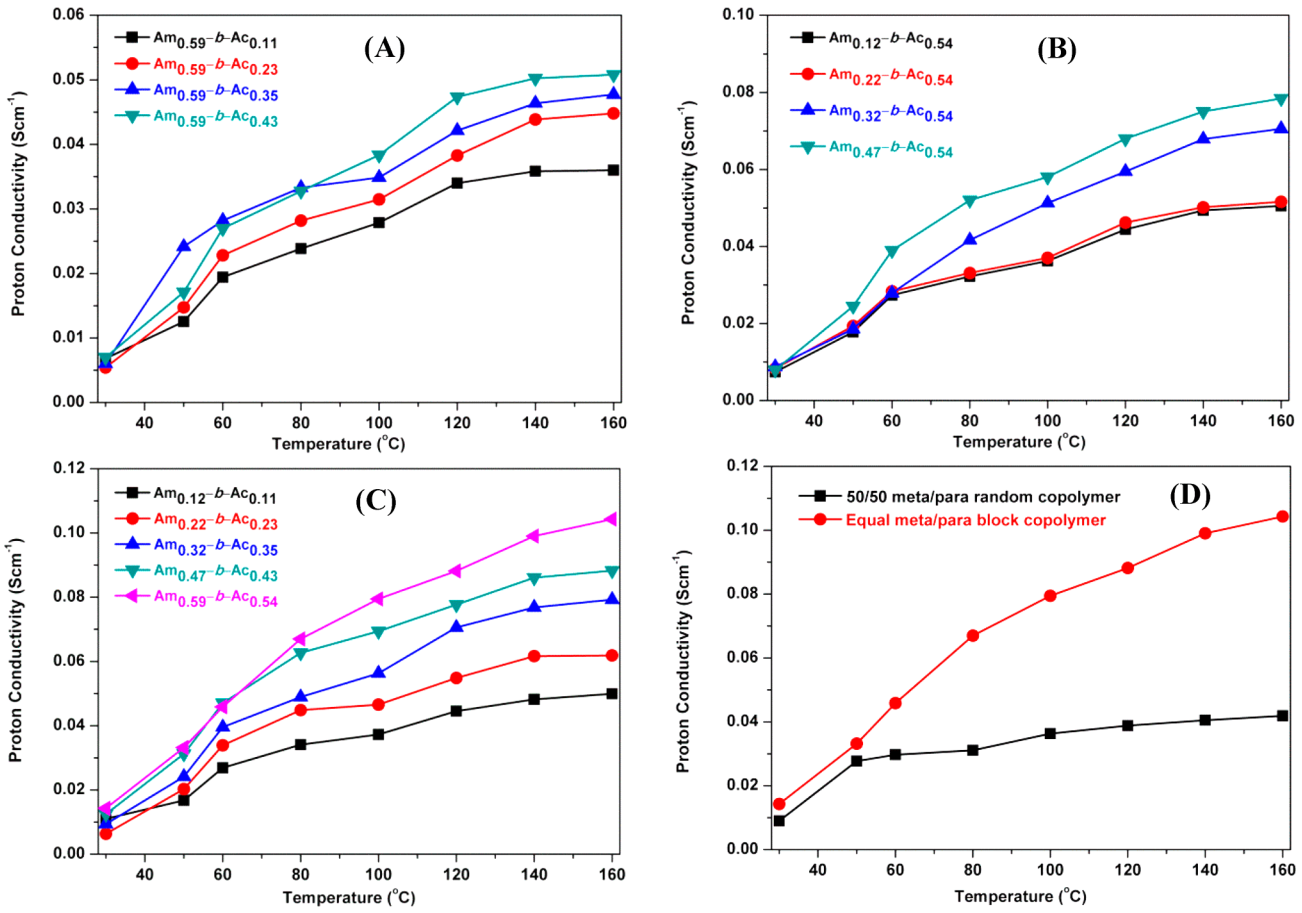


**Figure 7.** Proton conductivity plots of acid-doped segmented block PBI membranes against temperature without any external humidification supply: (A) fixed diamine terminated with varied acid terminated ($Am_{fix}$-*b*-$Ac_{vary}$), (B) fixed acid terminated with varied diamine terminated ($Am_{vary}$-*b*-$Ac_{fix}$), (C) equal diamine and acid terminated ($Am_{equal}$-*b*-$Ac_{equal}$) block copolymer, and (D) comparison of segmented block and random copolymers. These membranes were obtained by doping the copolymer membranes in 85% (14.6 M) $H_3PO_4$ for 7 days.


dx.doi.org/10.1021/am500668c | ACS Appl. Mater. Interfaces 2014, 6, 6851−6864

this symmetrical influence of para is completely disturbed by meta owing to the random distribution of meta and para structures in the PBI backbone and hence conductivity of 50/50 meta/para random copolymer decreases. However, in case of blocky structure, since phase separated morphology of meta and para structures are resulted and hence the interference by the meta to para is reduced which resulted in increased connectivity within para PBI units. This connnectivity between the para increases with increasing block length which in turn lowered the morphological barrier between the para segments resulting higher conductivity despite the similar PA loading. On the other hand in case of random copolymer because of phase mixing the high morphological barrier sets in which in turn reduces the proton conductivity.

It must be noted from Figure 7 that there are significant differences in the increase in proton conductivity from one type block structure to another, these are may be due to the structural effect which influences the nanophase separation of these block copolymers.

## CONCLUSION

A series of polybenzimidazole (PBI) segmented block copolymers namely *meta*-polybenzimidazole-*block*-*para*-polybenzimidazole (*m*-PBI-*b*-*p*-PBI) of three different structural varieties are synthesized with an aim to develop new type of PBI based polymer electrolyte membrane (PEM). The segmented block copolymers of PBI are synthesized by condensing diamine terminated meta-oriented polybenzimidazole (*m*-PBI-Am) and acid terminated para-oriented polybenzimidazole (*p*-PBI-Ac) oligomers. The block length and the structural motifs of the segmented block copolymers are diversified by choosing and optimizing the appropriate pairs of oligomers with targeted molecular weight. Extensive NMR studies confirmed the formation of segmented block copolymers of varieties of structures, which was also supported by DMA studies. Thermally and mechanically stable membrane prepared by solvent casting from methanesulfonic acid (MSA) solution of polymers displayed two $T_g$ values in DMA studies confirming the formation of segmented block copolymer structure. The existence of nanophase separation between two blocks is confirmed from the DMA studies. Increase in block length decreases the phase mixing between two blocks, which in turn facilitated the nanophase segregation of two blocks: this is confirmed from the observation of DMA studies that $T_g$ peaks for higher block length copolymers increasingly become more distinct. Phosphoric acid loading of the segmented block copolymers does not follow any trends as a function of block length or the copolymer structural motifs. On the other hand, proton conductivities for all the copolymers increase with increasing block length because of the increased phase separation which improved the connectivity within the same block and hence increase the conductivity. The block structural motif also influences the proton conductivity. A comparison of segmented block copolymers with random meta/para copolymers clearly indicates that the former exhibit much higher proton conductivity in the similar $H_3PO_4$ loading, attributing that new block copolymers are much better alternative as PBI-based PEM.

## ASSOCIATED CONTENT

### Supporting Information

Materials sources, experimental details for all characterization methods, double logarithm plot inherent viscosity vs number-average molecular weights of oligomers, TGA plots of oligomers, tan $\delta$ vs temperature plots of block copolymers, and Nyquist plots of proton conduction measurements of the PA-doped PBI block copolymers membranes. This material is available free of charge via the Internet at http://pubs.acs.org.

## AUTHOR INFORMATION

### Corresponding Author

*Tel: (91) 40 23134808. Fax: (91) 40 23012460. E-mail: tusharjana@uohyd.ac.in, tjscuoh@gmail.com.

### Notes

The authors declare no competing financial interest.

## ACKNOWLEDGMENTS

We gratefully acknowledge the financial support by DST (Grant No. SR/SI/PC58/2008). S. M. thanks UGC for the junior and senior research fellowship.

## REFERENCES

(1) Li, Q.; Jensen, J. O.; Savinell, R. F.; Bjerrum, N. J. High-Temperature Proton Exchange Membranes Based on Polybenzimidazoles for Fuel Cells. *Prog. Polym. Sci.* **2009**, *34*, 449−477.

(2) Asensio, J. A.; Sánchez, E. M.; Gómez-Romer, P. Proton-Conducting Membranes Based on Benzimidazole Polymers for High-Temperature PEM Fuel Cells. *Chem. Soc. Rev.* **2010**, *39*, 3210−3239.

(3) Mader, J.; Xiao, L.; Schmidt, T. J.; Benicewicz, B. C. Polybenzimidazole/Acid Complexes as High-Temperature Membranes. *Adv. Polym. Sci.* **2008**, *216*, 63−124.

(4) Zhang, H.; Shen, P. K. Recent Development of Polymer Electrolyte Membranes for Fuel Cells. *Chem. Rev.* **2012**, *112*, 2780−2832.

(5) Hickner, M. A.; Ghassemi, H.; Kim, S. Y.; Einsla, B. R.; McGrath, J. E. Alternative Polymer Systems for Proton Exchange Membranes (PEMs). *Chem. Rev.* **2004**, *104*, 4587−4612.

(6) Parka, C. H.; Leeb, C. H.; Guivera, M. D.; Lee, Y. M. Sulfonated Hydrocarbon Membranes for Medium-Temperature and Low-Humidity Proton Exchange Membrane Fuel Cells (PEMFCs). *Prog. Polym. Sci.* **2011**, *36*, 1443−1498.

(7) Celik, S. U.; Bozkurta, A.; Hosseini, S. S. Alternatives toward Proton Conductive Anhydrous Membranes for Fuel Cells: Heterocyclic Protogenic Solvents Comprising Polymer Electrolytes. *Prog. Polym. Sci.* **2012**, *37*, 1265−1291.

(8) Weber, J.; Antonietti, M.; Thomas, A. Mesoporous Poly(Benzimidazole) Networks via Solvent Mediated Templating of Hard Spheres. *Macromolecules* **2007**, *40*, 1299−1304.

(9) Mader, J. A.; Benicewicz, B. C. Sulfonated Polybenzimidazoles for High-Temperature PEM Fuel Cells. *Macromolecules* **2010**, *43*, 6706−6715.

(10) Kim, S.-K.; Choi, S.-W.; Jeon, W. S.; Park, J. O.; Ko, T.; Chang, H.; Lee, J.-C. Cross-Linked Benzoxazine-Benzimidazole Copolymer Electrolyte Membranes for Fuel Cells at Elevated Temperature. *Macromolecules* **2012**, *45*, 1438−1446.

(11) Pu, H.; Wang, L.; Pan, H.; Wan, D. Synthesis and Characterization of Fluorine-Containing Polybenzimidazole for Proton Conducting Membranes in Fuel Cells. *J. Polym. Sci., Part A: Polym. Chem.* **2010**, *48*, 2115−2122.

(12) Xiao, L.; Zhang, H.; Scanlon, E.; Ramanathan, L. S.; Choe, E.-W.; Rogers, D.; Apple, T.; Benicewicz, B. C. High-Temperature Polybenzimidazole Fuel Cell Membranes via a Sol−Gel Process. *Chem. Mater.* **2005**, *17*, 5328−5333.

(13) Wang, S.; Zhao, C.; Ma, W.; Zhang, N.; Zhang, Y.; Zhang, G.; Liu, Z.; Na, H. Silane-Cross-Linked Polybenzimidazole with Improved Conductivity for High Temperature Proton Exchange Membrane Fuel Cells. *J. Mater. Chem. A* **2013**, *1*, 621−629.

(14) Maity, S.; Jana, T. *N*-Alkyl Polybenzimidazole: Effect of Alkyl Chain Length. *Eur. Polym. J.* **2013**, *49*, 2280−2292.

(15) Klaehn, J. R.; Luther, T. A.; Orme, C. J.; Jones, M. G.; Wertsching, A. K.; Peterson, E. S. Soluble N-Substituted Organosilane Polybenzimidazoles. *Macromolecules* **2007**, *40*, 7487−7492.

(16) Weber, J.; Kreuer, K.-D.; Maier, J.; Thomas, A. Proton Conductivity Enhancement by Nanostructural Control of Poly-(Benzimidazole)−Phosphoric Acid Adducts. *Adv. Mater.* **2008**, *20*, 2595−2598.
(17) Glipa, X.; Bonnet, B.; Mula, B.; Jones, D. J.; Roziere, J. Investigation of the Conduction Properties of Phosphoric and Sulfuric Acid-Doped Polybenzimidazole. *J. Mater. Chem.* **1999**, *9*, 3045−3049.
(18) Mustarelli, P.; Quartarone, E.; Grandi, S.; Carollo, A.; Magistris, A. Polybenzimidazole-Based Membranes as a Real Alternative to Nafion for Fuel Cells Operating at Low Temperature. *Adv. Mater.* **2008**, *20*, 1339−1343.
(19) Berber, M. R.; Fujigaya, T.; Sasaki, K.; Nakashima, N. Remarkably Durable High Temperature Polymer Electrolyte Fuel Cell Based on Poly(Vinylphosphonic acid)-Doped Polybenzimidazole. *Sci. Rep.* **2013**, *3*, 1764−1770.
(20) Carollo, A.; Quartarone, E.; Tomasi, C.; Mustarelli, P.; Belotti, F.; Magistris, A.; Maestroni, F.; Parachini, M.; Garlaschelli, L.; Righetti, P. P. Developments of New Proton Conducting Membranes Based on Different Polybenzimidazole Structures for Fuel Cells Applications. *J. Power Sources* **2006**, *160*, 175−180.
(21) Gieselman, M. B.; Reynolds, J. R. Water-Soluble Polybenzimidazole-Based Polyelectrolytes. *Macromolecules* **1992**, *25*, 4832−4834.
(22) Pu, H.; Liu, Q.; Liu, G. Methanol Permeation and Proton Conductivity of Acid-Doped Poly(*N*-Ethylbenzimidazole) and Poly-(*N*-Methylbenzimidazole). *J. Membr. Sci.* **2004**, *241*, 169−175.
(23) Glipa, X.; Haddad, M. E.; Jones, D. J.; Roziér, J. Synthesis and Characterisation of Sulfonated Polybenzimidazole: A Highly Conducting Proton Exchange Polymer. *Solid State Ionics* **1997**, *97*, 323−331.
(24) Kumbharkar, S. C.; Kharul, U. K. New N-Substituted ABPBI: Synthesis and Evaluation of Gas Permeation Properties. *J. Membr. Sci.* **2010**, *360*, 418−425.
(25) Angioni, S.; Righetti, P. P.; Quartarone, E.; Dilena, E.; Mustarelli, P.; Magistris, A. Novel Aryloxy-Polybenzimidazoles as Proton Conducting Membranes for High Temperature PEMFCs. *Int. J. Hydrogen Energy* **2011**, *36*, 7174−7182.
(26) Maity, S.; Jana, T. Soluble Polybenzimidazoles for PEM: Synthesized from Efficient, Inexpensive, Readily Accessible Alternative Tetraamine Monomer. *Macromolecules* **2013**, *46*, 6814−6823.
(27) Chuang, S. W.; Hsu, S. L. C. Synthesis and Properties of a New Fluorine-Containing Polybenzimidazole for High-Temperature Fuel-Cell Applications. *J. Polym. Sci., Part A: Polym. Chem.* **2006**, *44*, 4508−4513.
(28) Qing, S.; Huang, W.; Yan, D. Synthesis and Characterization of Thermally Stable Sulfonated Polybenzimidazoles Obtained from 3,3′-Disulfonyl-4,4′-Dicarboxyldiphenylsulfone. *J. Polym. Sci., Part A: Polym. Chem.* **2005**, *43*, 4363−4372.
(29) Yang, J.; Xu, Y.; Zhou, L.; Che, Q.; He, R.; Li, Q. Hydroxyl Pyridine Containing Polybenzimidazole Membranes for Proton Exchange Membrane Fuel Cells. *J. Membr. Sci.* **2013**, *446*, 318−325.
(30) Sannigrahi, A.; Ghosh, S.; Maity, S.; Jana, T. Structurally Isomeric Monomers Directed Copolymerization of Polybenzimidazoles and Their Properties. *Polymer* **2010**, *51*, 5929−5941.
(31) Sannigrahi, A.; Arunbabu, D.; Sankar, R. M.; Jana, T. Tuning the Molecular Properties of Polybenzimidazole by Copolymerization. *J. Phys. Chem. B* **2007**, *111*, 12124−12132.
(32) Qian, G.; Benicewicz, B. C. Synthesis and Characterization of High Molecular Weight Hexafluoroisopropylidene-Containing Polybenzimidazole for High-Temperature Polymer Electrolyte Membrane Fuel Cells. *J. Polym. Sci., Part A: Polym. Chem.* **2009**, *47*, 4064−4073.
(33) Sannigrahi, A.; Arunbabu, D.; Jana, T. Thermoreversible Gelation of Polybenzimidazole in Phosphoric Acid. *Macromol. Rapid Commun.* **2006**, *27*, 1962−1967.
(34) Sannigrahi, A.; Ghosh, S.; Maity, S.; Jana, T. Polybenzimidazole Gel Membrane for the use in Fuel Cell. *Polymer* **2011**, *52*, 4319−4330.
(35) Mecerreyes, D.; Grande, H.; Miguel, O.; Ochoteco, E.; Marcilla, R.; Cantero, I. Porous Polybenzimidazole Membranes Doped with Phosphoric Acid: Highly Proton-Conducting Solid Electrolytes. *Chem. Mater.* **2004**, *16*, 604−607.
(36) Xiao, L.; Zhang, H.; Jana, T.; Scanlon, E.; Chen, R.; Choe, E.-W.; Ramanathan, L. S.; Yu, S.; Benicewicz, B. C. Synthesis and Characterization of Pyridine-Based Polybenzimidazoles for High Temperature Polymer Electrolyte Membrane Fuel Cell Applications. *Fuel Cells* **2005**, *5*, 287−295.
(37) Shen, C.-H.; Jheng, L.-C.; Hsu, S. L. C.; Wang, J. T. W. Phosphoric Acid-Doped Cross-Linked Porous Polybenzimidazole Membranes for Proton Exchange Membrane Fuel Cells. *J. Mater. Chem.* **2011**, *21*, 15660−15665.
(38) Ghosh, S.; Sannigrahi, A.; Maity, S.; Jana, T. Role of Clays Structures on the Polybenzimidazole Nanocomposites: Potential Membranes for the Use in Polymer Electrolyte Membrane Fuel Cell. *J. Phys. Chem. C* **2011**, *115*, 11474−11483.
(39) Ghosh, S.; Sannigrahi, A.; Maity, S.; Jana, T. Polybenzimidazole/Silica Nanocomposites: Organic−Inorganic Hybrid Membranes for PEM Fuel Cell. *J. Mater. Chem.* **2011**, *21*, 14897−14906.
(40) Kannan, R.; Kagaiwale, H. N.; Chaudhari, H. D.; Kharul, U. K.; Kurungot, S.; Pillai, V. K. Improved Performance of Phosphonated Carbon Nanotube−Polybenzimidazole Composite Membranes in Proton Exchange Membrane Fuel Cells. *J. Mater. Chem.* **2011**, *21*, 7223−7231.
(41) Chung, S.-W.; Hsu, S. L.-C.; Liu, Y.-H. Synthesis and Properties of Fluorine-Containing Polybenzimidazole/Silica Nanocomposite Membranes for Proton Exchange Membrane Fuel Cells. *J. Membr. Sci.* **2007**, *305*, 353−363.
(42) Deimede, V.; Voyiatzis, G. A.; Kallitsis, J. K.; Qingfeng, L.; Bjerrum, J. N. Miscibility Behavior of Polybenzimidazole/Sulfonated Polysulfone/Blends for Use in Fuel Cell Applications. *Macromolecules* **2000**, *33*, 7609−7617.
(43) Arunbabu, D.; Sannigrahi, A.; Jana, T. Blends of Polybenzimidazole and Poly(Vinylidene Fluoride) for Use in a Fuel Cell. *J. Phys. Chem. B* **2008**, *112*, 5305−5310.
(44) Hazarika, M.; Jana, T. Proton Exchange Membrane Developed from Novel Blends of Polybenzimidazole and Poly(Vinyl-1,2,4-triazole). *ACS Appl. Mater. Interfaces* **2012**, *4*, 5256−5265.
(45) Hazarika, M.; Jana, T. Novel Proton Exchange Membrane for Fuel Cell Developed from Blends of Polybenzimidazole with Fluorinated Polymer. *Eur. Polym. J.* **2013**, *49*, 1564−1576.
(46) Qing, S.; Huang, W.; Yan, D. Synthesis and Characterization of Thermally Stable Sulfonated Polybenzimidazoles. *Eur. Polym. J.* **2005**, *41*, 1589−1595.
(47) Jouanneau, J.; Mercier, R.; Gonon, L.; Gebel, G. Synthesis of Sulfonated Polybenzimidazoles from Functionalized Monomers: Preparation of Ionic Conducting Membranes. *Macromolecules* **2007**, *40*, 983−990.
(48) Jouanneau, J.; Gonon, L.; Gebel, G.; Martin, V.; Mercier, R. Synthesis and Characterization of Ionic Conducting Sulfonated Polybenzimidazoles. *J. Polym. Sci., Part A: Polym. Chem.* **2010**, *48*, 1732−1742.
(49) Yang, J.; He, R.; Che, Q.; Gao, X.; Shi, L. A Copolymer of Poly[2,2′-(M-Phenylene)-5,5′-Bibenzimidazole] and Poly(2,5-Benzimidazole) for High-Temperature Proton-Conducting Membranes. *Polym. Int.* **2010**, *59*, 1695−1700.
(50) Yu, S.; Benicewicz, B. C. Synthesis and Properties of Functionalized Polybenzimidazoles for High-Temperature PEMFCs. *Macromolecules* **2009**, *42*, 8640−8648.
(51) Seel, D. C.; Benicewicz, B. C. Polyphenylquinoxaline-Based Proton Exchange Membranes Synthesized via the PPA Process for High Temperature Fuel Cell Systems. *J. Membr. Sci.* **2012**, *405*, 57−67.
(52) Kulkarni, M. P.; Peckham, T. J.; Thomas, O. D.; Holdcroft, S. Synthesis of Highly Sulfonated Polybenzimidazoles by Direct Copolymerization and Grafting. *J. Polym. Sci., Part A: Polym. Chem.* **2013**, *51*, 3654−3666.
(53) Elabd, Y. A.; Hickner, M. A. Block Copolymers for Fuel Cells. *Macromolecules* **2011**, *44*, 1−11.
(54) Harrison, W. L.; Hickner, M. A.; Kim, Y. S.; McGrath, J. E. Poly(Arylene Ether Sulfone) Copolymers and Related Systems from Disulfonated Monomer Building Blocks: Synthesis, Characterization, and Performance-A Topical Review. *Fuel Cells* **2005**, *5*, 201−212.

(55) Wang, H.; Badami, A. S.; Roy, A.; McGrath, J. E. Multiblock Copolymers of Poly(2,5-Benzophenone) and Disulfonated Poly(Arylene Ether Sulfone) for Proton-Exchange Membranes. I. Synthesis and Characterization. *J. Polym. Sci., Part A: Polym. Chem.* **2007**, *45*, 284−294.
(56) Chen, Y.; Guo, R.; Lee, C. H.; Lee, M.; McGrath, J. E. Partly Fluorinated Poly(Arylene Ether Ketone Sulfone) Hydrophilic−Hydrophobic Multiblock Copolymers for Fuel Cell Membranes. *Int. J. Hydrogen Energy* **2012**, *37*, 6132−6139.
(57) Lee, H. S.; Roy, A.; Lane, O.; McGrath, J. E. Synthesis and Characterization of Poly(Arylene Ether Sulfone)-*b*-Polybenzimidazole Copolymers for High Temperature Low Humidity Proton Exchange Membrane Fuel Cells. *Polymer* **2008**, *49*, 5387−5396.
(58) Ng, F.; Bae, B.; Miyatake, K.; Watanabe, M. Polybenzimidazole Block Sulfonated Poly(Arylene Ether Sulfone) Ionomers. *Chem. Commun.* **2011**, *47*, 8895−8897.
(59) Mader, J. A.; Benicewicz, B. C. Synthesis and Properties of Segmented Block Copolymers of Functionalised Polybenzimidazoles for High-Temperature PEM Fuel Cells. *Fuel Cells* **2011**, *11*, 222−237.
(60) Asensio, J. A.; Borros, S.; Gomez-Romero, P. Polymer Electrolyte Fuel Cells Based on Phosphoric Acid-Impregnated Poly(2,5-Benzimidazole) Membranes. *J. Electrochem. Soc.* **2004**, *151*, A304−A310.